Title:

An immunodominance hierarchy exists in $CD8^+$ T cell responses to HLA-A*02:01-restricted epitopes identified from the non-structural polyprotein 1a of SARS-CoV-2.

Running title:

Dominant hierarchy of CTL epitopes in SARS-CoV-2 pp1a

Authors:

Akira Takagi,[1] and Masanori Matsui[2]*

Affiliation:

[1]School of Medical Technology, Faculty of Health and Medical Care, Saitama Medical University, 1397-1 Yamane, Hidaka-city, Saitama 350-1241, Japan

[2]Department of Microbiology, Faculty of Medicine, Saitama Medical University, 38 Morohongo, Moroyama-cho, Iruma-gun, Saitama 350-0495, Japan

*Corresponding author. E-mail address: mmatsui@saitama-med.ac.jp

Tel: +81-49-276-1438; Fax: +81-49-295-9107.

Key words:

SARS-CoV-2, COVID-19, CTL epitope, HLA-A*02:01, pp1a, vaccine, immunodominance, hierarchy

Abstract

COVID-19 vaccines are being rapidly developed and human trials are underway. Almost all of these vaccines have been designed to induce antibodies targeting spike protein of SARS-CoV-2 in expectation of neutralizing activities. However, non-neutralizing antibodies are at risk of causing antibody-dependent enhancement. Further, the longevity of SARS-CoV-2-specific antibodies is very short. Therefore, in addition to antibody-induced vaccines, novel vaccines on the basis of SARS-CoV-2-specific cytotoxic T lymphocytes (CTLs) should be considered in the vaccine development. Here, we attempted to identify HLA-A*02:01-restricted CTL epitopes derived from the non-structural polyprotein 1a of SARS-CoV-2. Eighty-two peptides were firstly predicted as epitope candidates on bioinformatics. Fifty-four in 82 peptides showed high or medium binding affinities to HLA-A*02:01. HLA-A*02:01 transgenic mice were then immunized with each of the 54 peptides encapsulated into liposomes. The intracellular cytokine staining assay revealed that 18 out of 54 peptides were CTL epitopes because of the induction of IFN-γ-producing $CD8^+$ T cells. In the 18 peptides, 10 peptides were chosen for the following analyses because of their high responses. To identify dominant CTL epitopes, mice were immunized with liposomes containing the mixture of the 10 peptides. Some peptides were shown to be statistically predominant over the other peptides. Surprisingly, all mice immunized with the liposomal 10 peptide mixture did not show the same reaction pattern to the 10 peptides. There were three pattern types that varied sequentially, suggesting the existence of an

immunodominance hierarchy, which may provide us more variations in the epitope selection for designing CTL-based COVID-19 vaccines.

Importance

For the development of vaccines based on SARS-CoV-2-specific cytotoxic T lymphocytes (CTLs), we attempted to identify HLA-A*02:01-restricted CTL epitopes derived from the non-structural polyprotein 1a of SARS-CoV-2. Out of 82 peptides predicted on bioinformatics, 54 peptides showed good binding affinities to HLA-A*02:01. Using HLA-A*02:01 transgenic mice, 18 in 54 peptides were found to be CTL epitopes in the intracellular cytokine staining assay. Out of 18 peptides, 10 peptides were chosen for the following analyses because of their high responses. To identify dominant epitopes, mice were immunized with liposomes containing the mixture of the 10 peptides. Some peptides were shown to be statistically predominant. Surprisingly, all immunized mice did not show the same reaction pattern to the 10 peptides. There were three pattern types that varied sequentially, suggesting the existence of an immunodominance hierarchy, which may provide us more variations in the epitope selection for designing CTL-based COVID-19 vaccines.

Introduction

In December 2019, the coronavirus disease 2019 (COVID-19) caused by the severe acute respiratory syndrome coronavirus 2 (SARS-CoV-2) was firstly identified in Wuhan, Hubei province, China. Since then, its subsequent spread of global infection has still continued to gain momentum. As of September 16th, 2020, the COVID-19 pandemic has infected more than 29.4 million people around the world and caused more than 931,000 deaths. Although the clinical symptom is varied from asymptomatic or mild self-limited infection to severe life-threating respiratory disease, the mechanism of disease outcome remains unclear. Many nations are struggling to find appropriate preventive and control strategies. However, there are no vaccines or antiviral drugs available for the treatment of this infectious disease.

There are seven coronaviruses that infect humans. In addition to SARS-CoV-2, SARS-CoV and middle-east respiratory syndrome coronavirus (MERS-CoV) cause severe pneumonia, whereas the other four human coronaviruses including HCoV-229E, -NL63, -OC43 and -HKU1 cause common cold (1). Like other coronaviruses, SARS-CoV-2 possesses a large single-stranded positive sense RNA genome (2). As shown in Fig. 1, the 5'-terminal two-thirds of the genome are composed of ORF1a and ORF1b. ORF1a encodes the polyprotein 1a (pp1a) containing non-structural proteins (nsp1-11) (Fig. 1). The remaining one-third of the genome encodes the structural proteins involving spike (S), envelope (E), membrane (M), and nucleocapsid (N) as well as accessory proteins (Fig. 1). Coronaviruses depend on S protein for binding to host cells.

The host cell receptor for SARS-CoV-2 is the angiotensin-converting enzyme 2 (ACE2) which is also the receptor for SARS-CoV (3, 4).

It was shown that the increased cell numbers of antibody-secreting cells, follicular helper T cells, activated $CD4^+$ T cells and $CD8^+$ T cells were observed in a non-severe COVID-19 patient (5), indicating that robust immune responses can be elicited to the newly emerged, SARS-CoV-2. Therefore, the induction of protective immunity against SARS-CoV-2 is considered to help control COVID-19. Vaccines are being rapidly developed in the world, and human trials are underway for several vaccine candidates, ranging from traditional vaccines comprised of inactivated SARS-CoV-2 preparations (6) to innovative vaccines such as subunit (7), RNA (8), DNA (9), and adenoviral (10) vaccines. Almost all of these vaccines have been designed to induce antibodies targeting S protein because some antibodies specific for the receptor binding domain (RBD) of S protein may have neutralizing activities and can interfere with the binding between ACE2 on host cells and virus. In fact, it was reported that DNA vaccine encoding S protein induced neutralizing antibody in rhesus macaques and protected them from the challenge with SARS-CoV-2 (9). However, there are two major issues concerning this vaccine. One issue is that non-neutralizing and sub-neutralizing antibodies to S protein induced by this vaccine are at risk of causing antibody-dependent enhancement (ADE) (11). ADE is the phenomenon in which binding of suboptimal antibodies to viruses enhances viral entry mediated by Fc receptors into immune cells, and promotes inflammatory and tissue injury (12). ADE has been reported in the evaluation of vaccine candidates directed to S protein

for SARS-CoV (13-16). Because of their similarities, these findings enable us to foresee the high risks of ADE in SARS-CoV-2 vaccines directed to S protein. It is worth noting that RBD-specific antibodies with potent neutralizing activity are extremely rare among S-specific antibodies in COVID-19-covalescent individuals (17, 18), suggesting that the development of effective vaccines might requires novel strategies to selectively target RBD of SARS-CoV-2. On the other hand, Passive immunization of RBD-specific monoclonal antibodies obtained from convalescent individuals might be safe and effective for the elimination of SARS-CoV-2 (19-21), but much more expensive to produce for worldwide use than vaccines (22). The other issue is the short longevity of neutralizing antibodies to SARS-CoV-2. It was previously reported that the SARS-CoV-specific antibodies are short-lived for at most about 2-3 years (23, 24) in comparison with SARS-CoV-specific memory T cells (25). The longevity of SARS-CoV-2-specific antibodies are likely to be even shorter, as indicated by antibody titers being undetectable or approaching baseline in the majority of SARS-CoV-2-infected individuals after 2-3 months post onset of symptoms (26). Taken together, these data strongly suggest that it does not seem right to rely too much on just the S-specific antibody-induced vaccine to control the COVID-19 pandemic.

In the viral infection, $CD8^+$ cytotoxic T lymphocytes (CTLs) play an important role for the clearance of virus as well as neutralizing antibodies. CTLs recognize virus-derived peptides in association with major histocompatibility complex class I (MHC-I) molecules on the surface of antigen presenting cells and kill virus-infected target cells. It was

126 reported that $CD4^+$ T cells and $CD8^+$ T cells are decreased in proportion to the disease
127 severity and are exhausted in severe COVID-19 patients (27, 28), suggesting the
128 significance of $CD8^+$ CTLs in the clearance of SARS-CoV-2. Furthermore,
129 SARS-CoV-specific memory T cells persisted up to 11 years (25), predicting the long life
130 of SARS-CoV-2-specific memory T cells. Therefore, in addition to antibody-induced
131 vaccines, novel vaccines based on SARS-CoV-2-specific CTLs should also be considered
132 in the future vaccine development for the prevention and disease control of COVID-19.
133 For the development of CTL-based COVID-19 vaccine, we here attempted to identify
134 HLA-A*02:01-restricted, dominant CTL epitopes derived from pp1a of SARS-CoV-2.
135 Pp1a is a largest protein composed of 4,401 amino acids among SARS-CoV-2 proteins,
136 and therefore, it seems highly possible to find dominant epitopes in this protein.
137 Furthermore, pp1a is produced first in SARS-CoV-2-infected cells, suggesting
138 pp1a-specific CTLs could kill infected cells before the formation of mature virions. In
139 addition, this protein is composed of 11 non-structural regulatory proteins that are highly
140 conserved among many different coronaviruses (29). To identify CTL epitopes, we used
141 computational algorithms, HLA-A*02:01 transgenic mice and the peptide-encapsulated
142 liposomes. In a similar way, we previously identified CTL epitopes of SARS-CoV pp1a
143 (30).
144

Results

Prediction of HLA-A*02:01-restricted CTL epitopes derived from SARS-CoV-2 pp1a.

We firstly attempted to predict HLA-A*02:01-restricted CTL epitopes derived from SARS-CoV-2 pp1a using four computer-based programs, SYFPEITHI (31), nHLAPred (32), ProPred-I (33), and IEDB (34). Eighty-two epitopes with high scores for all four programs were selected and synthesized into 9-mer peptides (Table 1). These peptides were then evaluated for their binding affinities to HLA-A*02:01 molecule using TAP2-deficient RMA-S-HHD cells. As the half-maximal binding level (BL_{50}) values of the influenza A virus matrix protein 1-derived peptide, FMP_{58-66} (35) as a high binder control and the HIV reverse transcriptase-derived peptide, HIV-$pol_{476-484}$ (36) as a medium binder control were 2.3 μM and 80.6 μM, respectively, we defined a high binder with a BL_{50} value below 10 μM, a medium binder with a BL_{50} value ranging from 10 to 100 μM, and a low binder with a BL_{50} value above 100 μM. As shown in Table 1, 20 peptides were high binders, whereas 34 peptides were medium binders, suggesting that the bioinformatics prediction was mostly successful. In contrast, the remaining 28 peptides displayed low affinities or no binding to HLA-A*02:01 molecules (Table 1). In the following experiments, 54 peptides involving high binders and medium binders were chosen to further investigate their abilities of peptide-specific CTL induction.

Detection of SARS-CoV-2 pp1a-specific CD8$^+$ T cell responses in mice immunized with peptide-encapsulated liposomes.

Each of 54 peptides selected were encapsulated into liposomes as described in the materials and methods. HLA-A*02:01 transgenic (HHD) mice (37) were then subcutaneously (s.c.) immunized twice at a one-week interval with each of peptide-encapsulated liposomes together with CpG adjuvant. One week later, spleen cells of immunized mice were prepared, stimulated *in vitro* with a relevant peptide for 5 hours, and stained for their expression of cell-surface CD8 and intracellular interferon-gamma (IFN-γ). As shown in Fig. 2, the intracellular cytokine staining (ICS) assay showed that significant numbers of IFN-γ-producing CD8+ T cells were elicited in mice immunized with 18 liposomal peptides including pp1a-38, -52, -84, -103, -445, -597, -641, -1675, -2785, -2884, -3083, -3403, -3467, -3583, -3662, -3710, -3732, and -3886, revealing that these 18 peptides are HLA-A*02:01-restricted CTL epitopes derived from SARS-CoV-2 pp1a. As indicated in Table 2, multiple epitopes are located in small proteins such as nsp1 (180 aa) and nsp6 (290 aa), whereas only one epitope is seen in the large nsp3 composed of 1945 amino acids. On the other hand, the remaining 36 peptides out of 54 peptides in liposomes were not able to stimulate peptide-specific CTLs in mice (data not shown), demonstrating the necessity to generate data through wet-lab experiments. Interestingly, four epitopes including pp1a-103, -2884, -3403, and -3467 are located in the amino acid sequence of SARS-CoV pp1a as well (Table 2). pp1a-3467 was previously reported by us in the identification of SARS-CoV-derived CTL epitopes (30). However, any of 18

186 epitopes are not found in the amino acid sequence of either MERS-CoV or the four
187 common cold human coronaviruses involving HCoV-OC43, HCoV-229E, HCoV-NL63,
188 and HCoV-HKU1.

189 In the 18 positive peptides, 10 peptides including pp1a-38, -84, -641, -1675, -2884,
190 -3467, -3583, -3662, -3710, and -3732 were selected for the following analyses because
191 of the high ratios of IFN-γ^+ cells in $CD8^+$ T cells (Fig. 2).

192

193 **Identification of dominant CTL epitopes.**

194 To confirm that the 10 peptides are effective epitopes for peptide-specific CTL
195 responses, we examined whether peptide-specific killing activities were elicited in mice
196 with each of 10 peptides in liposomes. HHD mice were immunized s.c. twice with each
197 of peptide-encapsulated liposomes and CpG adjuvant. One week later, equal numbers of
198 peptide-pulsed and -unpulsed target cells were transferred into immunized mice via i.v.
199 injection, and peptide-specific lysis was analyzed by flow cytometry. In support of the
200 data of ICS (Fig. 2), peptide-specific killing was observed in mice immunized with any of
201 10 liposomal peptides (Fig. 3A).

202 We next attempted to identify dominant CTL epitopes among the 10 CTL epitopes.
203 The same amounts of the 10 peptide solutions at an equal concentration were mixed
204 together and encapsulated into liposomes. Seventeen mice were immunized once with the
205 liposomes containing the mixture of 10 peptides. One week later, spleen cells were
206 incubated with each of the 10 peptides for 5 hours, and the ICS assay was performed. As

shown in Fig. 3B & C, pp1a-38 and -84 were statistically predominant over almost all other peptides in the induction of peptide-specific IFN-γ^+ $CD8^+$ T cells. Furthermore, pp1a-641 and pp1a-3732 were significantly superior to pp1a-1675/-3583 and pp1a-1675/-3583/-3662 in the stimulation of IFN-γ-producing $CD8^+$ T cells, respectively (Fig. 3B).

We also examined the peptide-specific induction of $CD107a^+$ $CD8^+$ T cells and $CD69^+$ $CD8^+$ T cells. CD107a and CD69 are markers of degranulation and early activation on $CD8^+$ T lymphocytes, respectively. Nine mice were immunized once with the liposomes encapsulating the mixture of the 10 peptides. After one week, spleen cells were stimulated with each peptide, and stained for their expression of CD107a or CD69 of $CD8^+$ T cells. At first glance, the graphs of CD107a (Fig. 4A) and CD69 (Fig. 4B) expression were similar to that of IFN-γ expression of $CD8^+$ T cells (Fig. 3C). As shown in Figs. 4A & 4C, both pp1a-38 and pp1a-84 were superior to almost all other peptides for the CD107a expression of $CD8^+$ T cells. Moreover, pp1a-641 and pp1a-3732 elicited CD107a-positive T cells better than pp1a-1675/-2884/-3467 and pp1a-1675/-2884/-3467/-3583, respectively. In the case of CD69 expression (Figs. 4B & 4D), pp1a-38 and pp1a-3732 were more dominant than pp1a-1675/-2884/-3467/-3583 and pp1a-1675/-2884/-3467/-3583/-3662, respectively. Further, pp1a-84 was superior to pp1a-1675/-2884.

Taken together, 10 peptides differed significantly in their ability to induce SARS-CoV-2 pp1a-specific CTLs when mice were immunized with the mixture of 10

peptides in liposomes. Thus, some peptides were found to be dominant CTL epitopes although each peptide alone of the 10 peptides has the capability to efficiently activate peptide-specific CTL (Figs. 2 & 3A).

Existence of an immunodominance hierarchy.

The data in Fig. 5 indicate reactivity to the 10 peptides in each of 15 mice immunized with the mixture of the 10 peptides in liposomes. Each graph represents reactivity of an individual mouse (Fig. 5). Unexpectedly, all mice did not show the same reaction pattern against the 10 peptides. It looks like there were roughly three types that varied sequentially in terms of the reaction pattern to the 10 peptides. Type A is a group of mice in which pp1a-38, -84, -641-specific IFN-γ^+ $CD8^+$ T cells were predominantly elicited, whereas the remaining 7 peptides were not able to activate peptide-specific IFN-γ^+ $CD8^+$ T cells. In the case of type B, pp1a-3732 stimulated peptide-specific IFN-γ^+ $CD8^+$ T cells as well as pp1a-38, and -84. In addition to these three peptides, several other peptides also induced IFN-γ^+ $CD8^+$ T cells in Type C. These data suggest that there seems to be an immunodominance hierarchy composed of three stages in $CD8^+$ T cell responses to the 10 peptides. The immunodominance hierarchy may provide us more variations for designing CTL-based COVID-19 vaccines.

Discussion

After the epidemics of SARS and MERS, scientists have not succeeded yet in developing preventive or therapeutic vaccines available for re-emergence of them. In the SARS and MERS vaccine development, the full-length S protein or its S1 subunit have frequently been used as an antigen to produce anti-RBD neutralizing antibodies. However, these vaccine candidates provided partial protection against virus challenge in animal models accompanied by safety concerns such as ADE (1). Furthermore, antibody responses to coronaviruses rapidly wane following infection or immunization (23, 24, 26). Considering the above, it should be necessary to consider CTL-based vaccine against SARS-CoV-2 to provide robust long-lived T cell memory although neutralizing antibody responses are a primary vaccine target.

In the current study, we aimed to find HLA-A*02:01-resctricted CTL dominant epitopes derived from SARS-CoV-2. Dominant epitopes induce strong immune response to eliminate a certain pathogen fast and effectively, and also contribute to make the memory T cell pool. We focused on pp1a of SARS-CoV-2 to find out CTL epitopes because pp1a is a largest and conserved polyprotein among the constituent proteins. Further, pp1a is produced earlier than structural proteins, suggesting that pp1a-specific CTLs can eliminate infected cells before the formation of mature virions. To predict CTL epitopes, we utilized bioinformatics to select 82 peptides with high scores in four kinds of computer-based programs (Table 1). In the evaluation of peptide binding, 54 peptides showed high or medium binding affinities to HLA-A*02:01 molecules, whereas the

268 remaining 28 peptides displayed low binding affinities or no binding (Table 1). Out of
269 them, only eighteen peptides were found to be CTL epitopes. Hence, we have to keep in
270 mind that currently available algorithms have a limited ability to accurately predict CTL
271 epitopes although the bioinformatics approach is very useful to quickly predict a number
272 of epitopes in a large protein (38, 39).

273 Among 18 epitopes which we have identified in the current study, 4 epitopes including
274 pp1a-103, -2884, -3403, and -3467 are present in the amino acid sequence of SARS-CoV
275 pp1a (100% identity) (Table 2). Therefore, CTLs induced by these four epitopes could
276 work fine for the clearance of SARS-CoV as well. In support of this data, Le Bert et al.,
277 reported that long lasting memory T cells in SARS-recovered individuals cross-reacted to
278 N protein of SARS-CoV-2 (40). Recently, several studies found that
279 SARS-CoV-2-reactive $CD4^+$ and $CD8^+$ T cells were detected in a substantial proportion
280 of healthy donors who have never infected with SARS-CoV-2 or SARS-CoV (40-44). It
281 is most likely that these individuals were previously infected with one of the four human
282 coronaviruses (HCoV-229E, -NL63, -OC43 and -HKU1) that cause seasonal common
283 cold. Nelde et al. demonstrated evidence that the amino acid sequences of several
284 SARS-CoV-2 T cell epitopes recognized by unexposed individuals are similar to some
285 amino acid sequences in the four seasonal common cold human coronaviruses with
286 identities ranging from 10% to 89% (not 100% identity) (44). However, anyone has not
287 shown evidence that people with this cross-reactivity are less susceptible to COVID-19.
288 It may be also possible to assume that pre-existing T cell immunity might be detrimental

289 through mechanisms such as original antigenic sin or ADE (45). In the current data, any
290 of the 18 epitopes was not found in the amino acid sequences of the four human
291 coronaviruses, suggesting that effective common CTL epitopes derived from pp1a, if any,
292 might be very few.

293 Here, we focused on CTL epitopes restricted by HLA-A*02:01 which is the most
294 common HLA class I allele in the world, and used highly reactive HLA-A*02:01
295 transgenic mice, termed HHD mice (37). Although we can use lymphocytes of
296 SARS-CoV-2-infected individuals to identify CTL epitopes, there are mainly two
297 advantages to using HHD mice. First, a large amount of blood of patients is required for
298 examine many candidates of CTL epitopes, but any number of mice can be prepared for
299 this purpose. Second, when using patients' lymphocytes, we are only testing whether the
300 peptide candidates are recognized by memory CTLs. When using naïve mice, however,
301 we can find whether the epitope candidates are able to prime peptide-specific CTLs,
302 which may be a better criterion to judge them as vaccine antigens. It is supposed that the
303 efficient epitope for CTL recognition is not always efficient for CTL priming. However,
304 we should take into account that the immunogenic variation in HLA class I transgenic
305 mice may not be identical to that in humans because the antigen processing and
306 presentation differ between them.

307 In the previous studies, we used peptide-linked liposomes as an immunogen (30). The
308 surface-linked liposomal peptides were effective for peptide-specific CTL induction in
309 mice. However, attaching peptides to the surface of liposomes followed by purifying

them through the column is a fairly complicated process and time-consuming. In the current study, peptide-encapsulated liposomes were used as an immunogen. In contrast to the peptide-linked liposomes, the peptide-encapsulated liposomes are prepared by just mixing liposomes and the peptide. In addition, the peptide-encapsulated liposomes are able to prime peptide-specific CTLs in mice as efficiently as the peptide-linked liposomes. Liposome itself consisting of lipid bilayers is a very safe material for humans. Therefore, the peptide-encapsulated liposomes are considered to be promising as a CTL-based vaccine candidate.

Understanding the mechanism of immunodominance is obviously important for the development of effective vaccines. When mice were immunized with liposomes containing the mixture of 10 peptides, it was found that some peptides induced peptide-specific CTLs stronger than other peptides (Figs. 3 & 4). As shown in Figs. 3 & 4, pp1a-38 and -84 are considered to be relatively dominant in comparison with other peptides. In general, dominant epitope-specific CTLs are activated sooner and proliferate faster than subdominant epitope-specific CTLs. This immunodominance may be associated with the affinity of peptide to MHC-I molecules and the affinity of T-cell receptor (TCR) to the peptide-MHC-I complex. As shown in Table I, the peptide affinity of pp1a-84 to HLA-A*02:01 is very high (BL_{50} = 6.8 μM), while pp1a-38 is a medium binder (BL_{50} = 76.8 μM). Interestingly, the peptide affinity of pp1a-38 is lowest among the 10 peptides selected (Table I). These data suggest that the affinity of TCR to the peptide-MHC-I complex is critical for CTL immunodominance. In the selection of

antigenic epitopes for the CTL-based vaccine against SARS-CoV-2, dominant epitopes such as pp1a-38 and -84 should be chosen because they produce strong CTL response to eliminate virus-infected cells effectively. However, the immunological pressure exerted by dominant epitopes may allow the epitope sequences of SARS-CoV-2 to be mutated, and therefore, a vaccine containing multiple antigenic epitopes should be recommended for a successful COVID-19 vaccine.

It was surprising that all of the genetically identical mice did not show the same reactive pattern against the 10 peptides when they were immunized with liposomes containing the mixture of 10 peptides (Fig. 5). There were roughly three pattern types, A-C, that varied sequentially, suggesting the existence of an immunodominance hierarchy composed of three stages in $CD8^+$ T cell responses to the 10 peptides (Fig. 5). The differences among the three types might be explained by the timing of CTL expansion. In the type A, dominant peptides, pp1a-38, -84, and -641 presumably activated T cells more efficiently than the other peptides, and hence, dominant peptide-specific CTLs proliferate faster and curtail the expansion of CTLs specific for the other peptides. In the type B, it is considered that the expansion of dominant CTLs specific for pp1a-38, and -84 was delayed for some reason compared to that in type A, and thereby subdominant CTLs specific for pp1a-3732 could afford to expand. It is also thought that even non-dominant CTLs proliferated because the expansion of both dominant CTLs and subdominant CTLs in the type C was later than that in the type B. Although it is difficult to explain what caused difference in the timing of CTL expansion

among three reaction types, it should be important to find out what it is for the development of CTL-based peptide vaccine.

In summary, we have identified 18 kinds of HLA-A*02:01-restricted CTL epitopes derived from pp1a of SARS-CoV-2 using computational algorithms, HLA-A*02:01 transgenic mice and the peptide-encapsulated liposomes. Out of 18 epitopes, we have also found some dominant CTL epitopes such as pp1a-38 and -84. In the process of finding dominant epitopes, we showed the existence of an immunodominance hierarchy in $CD8^+$ T cell responses to these epitopes. The immunodominance hierarchy composed of multiple stages may offer us more variations in the epitope selection for designing CTL-based COVID-19 vaccines. These data may provide important information for further studies of T cell immunity in COVID-19 and the development of preventive and/or therapeutic CTL-based vaccines against SARS-CoV-2.

Materials and Methods

Prediction of CTL epitopes.

Four computer-based programs including SYFPEITHI (31), nHLAPred (32), ProPred-I (33), and IEDB (34) were used to predict HLA-A*02:01-restricted CTL epitopes derived from pp1a of SARS-CoV-2 (GenBank accession numbers: LC528232.1 & LC528233.1). As shown in Table 1, 82 peptides with superior scores were selected and were synthesized by Eurofins Genomics (Tokyo, Japan). Two control peptides, $FMP_{58\text{-}66}$ (sequence: GILFGVFTL) (35) and HIV-$pol_{476\text{-}484}$ (sequence: ILKEPVHGV) (36), were synthesized as well.

Mice.

We used HLA-A*02:01 transgenic mice (37) that express a transgenic HLA-A*02:01 monochain, designated as HHD, in which human β2-microglobulin is covalently linked to a chimeric heavy chain composed of HLA-A*02:01 (α1 and α2 domains) and $H\text{-}2D^b$ (α3, transmembrane, and cytoplasmic domains). Six- to ten-week-old mice were used for all experiments. Mice were housed in appropriate animal care facilities at Saitama Medical University, and were handled according to the international guideline for experiments with animals. This study was approved by the Animal Research Committee of Saitama Medical University.

Cell lines.

RMA-S-HHD is a TAP2-dificient mouse lymphoma cell line, RMA-S (H-2^b) transfected with the HHD gene (37). RMA-S-HHD was cultured in RPMI-1640 medium (Nacalai Tesque Inc., Kyoto, Japan) with 10% FCS (Biowest, Nuaille, France) and 500 μg/ml G418 (Nacalai Tesque Inc.)

Peptide binding assay.

Binding of peptides to the HLA-A*02:01 molecule was measured using RMA-S-HHD cells, as described (46). Briefly, RMA-S-HHD cells were pre-cultured overnight at 26ºC in a CO_2 incubator, and then pulsed with each peptide at various concentrations ranging from 0.01 μM to 100 μM for 1 hour at 26ºC. After 3 hours' incubation at 37ºC, peptide-pulsed cells were stained with anti-HLA-A2 monoclonal antibody, BB7.2 (47), followed by FITC-labeled goat anti-mouse IgG antibody (Sigma-Aldrich, St. Louis, MO). Mean fluorescence intensity (MFI) of HLA-A2 expression on the surface of RMA-S-HHD cells was measured by flow cytometry (FACSCanto™ II, BD Biosciences, Franklin Lakes, NJ), and standardized as the percent cell surface expression by the following formula: % relative binding = [{(MFI of cells pulsed with each peptide) – (MFI of cells incubated at 37ºC without a peptide)}/{(MFI of cells incubated at 26ºC without a peptide) – (MFI of cells incubated at 37ºC without a peptide)}] × 100. The concentration of each peptide that yields the 50% relative binding was calculated as the half-maximal binding level (BL_{50}). $FMP_{58\text{-}66}$ and HIV-$pol_{476\text{-}484}$ were used as control peptides.

Peptide-encapsulated liposomes.

Peptide-encapsulated liposomes were prepared using Lipocapsulater FD-U PL (Hygieia BioScience, Osaka, Japan) according to the manufacturer's instructions with a slight modification. In brief, each of 54 synthetic peptides was dissolved in DMSO at a final concentration of 10 mM. For the first screening, the same amounts of 4 to 5 kinds of 10 mM peptides were mixed to make a total 100 μl, which was then diluted with 1.9 ml of H_2O. For the second screening, 20 μl of each peptide at 10 mM was diluted to 2 ml with H_2O. For the identification of dominant epitopes among the 10 peptides selected, 20 μl of each of the 10 peptide solutions at a concentration of 10 mM was mixed together, and the total volume was increased to 2 ml by adding 1.8 ml of H_2O. The peptide solution was added into a vial of Lipocapsulater containing 10 mg of dried liposomes, and incubated for 15 min at room temperature. The resultant solution contains peptide-encapsulated liposomes.

Immunization.

Mice were immunized s.c. once or twice at a one-week interval with peptide-encapsulated liposomes (100 μl/mouse) together with CpG-ODN (5002: 5'-TCCATGACGTTCTTGATGTT-3', Hokkaido System Science, Sapporo, Japan) (5 μg/mouse) in the footpad.

Intracellular cytokine staining (ICS).

ICS was performed as described (30). In brief, after 1 wk following immunization, spleen cells were incubated with 50 μM of each peptide for 5 hours at 37ºC in the presence of brefeldin A (GolgiPlug™, BD Biosciences), and were stained with FITC-conjugated anti-mouse CD8 monoclonal antibody (mAb) (BioLegend, San Diego, CA). Cells were then fixed, permeabilized, and stained with phycoerythrin (PE)-conjugated rat anti-mouse IFN-γ mAb (BD Biosciences). After washing the cells, flow cytometric analyses were performed using flow cytometry (FACSCanto™ II, BD Biosciences).

Detection of CD107a and CD69 molecules on $CD8^+$ T cells.

For the detection of CD107a, spleen cells of immunized mice were incubated with 50 μM of each peptide for 6 hours at 37ºC in the presence of monensin (GolgiStop™, BD Biosciences) and 0.8 μg of FITC-conjugated anti-mouse CD107a mAb (BioLegend). Cells were then stained with PE-Cy5-conjugated anti-mouse CD8 mAb (BioLegend). For the examination of CD69 marker, spleen cells of immunized mice were stimulated with 50 μM of each peptide for 4 hours at 37ºC. Cells were then stained with PE-conjugated anti-mouse CD69 mAb (BioLegend) and FITC-conjugated anti-mouse CD8 mAb. Stained cells were analyzed by flow cytometry (FACSCanto™ II, BD Biosciences).

***In vivo* CTL assay.**

450 *In vivo* CTL assay was carried out as described (46). In brief, spleen cells from naive
451 HHD mice were equally split into two populations. One population was pulsed with 50
452 μM of a relevant peptide and labeled with a high concentration (2.5 μM) of
453 carboxyfluorescein diacetate succinimidyl ester (CFSE) (Molecular Probes, Eugene, OR).
454 The other population was unpulsed and labeled with a lower concentration (0.25 μM) of
455 CFSE. An equal number (1×10^7) of cells from each population was mixed together and
456 adoptively transferred i.v. into mice that had been immunized once with a liposomal
457 peptide. Sixteen hours later, spleen cells were prepared and analyzed by flow cytometry.
458 To calculate specific lysis, the following formula was used: % specific lysis =
459 [1-{(number of $CFSE^{low}$ cells in normal mice)/(number of $CFSE^{high}$ cells in normal
460 mice)}/{(number of $CFSE^{low}$ cells in immunized mice)/(number of $CFSE^{high}$ cells in
461 immunized mice)}] x 100.
462
463 **Statistical analyses.**
464 One-way ANOVA followed by post-hoc tests was performed for statistical analyses
465 among multiple groups using Graphpad Prism 5 software (GraphPad software, San
466 Diego, CA). A value of $P < 0.05$ was considered statistically significant.
467
468

ACKNOWLEDGMENTS

The authors are grateful to Professor François A. Lemonnier (Pasteur Institute, Paris, France) for providing HHD mice and RMA-S-HHD cells. This work was supported by a Grant-in-Aid for Scientific Research (C) (JSPS KAKENHI Grant Number: JP18K06631) to M. M., a Grant-in-Aid for Early-Career Scientists (JSPS KAKENHI Grant Number: JP18K15430) to A. T. from Japan Society for the Promotion of Science, and a Grant from Ochiai memorial award 2018 to A. T. The authors have no conflicting financial interests.

References

1. Sariol A, Perlman S. 2020. Lessons for COVID-19 immunity from other coronavirus infections. Immunity 53:248-263.

2. Srinivasan S, Cui H, Gao Z, Liu M, Lu S, Mkandawire W, Narykov O, Sun M, Korkin D. 2020. Structural genomics of SARS-CoV-2 indicates evolutionary conserved functional regions of viral proteins. Viruses 12:360. https://doi.org/10.3390/v12040360.

3. Walls AC, Park YJ, Tortorici MA, Wall A, McGuire AT, Veesler D. 2020. Structure, function, and antigenicity of the SARS-CoV-2 spike glycoprotein Cell 181:281-292.

4. Hoffmann M, Kleine-Weber H, Schroeder S, Krüger N, Herrler T, Erichsen S, Schiergens TS, Herrler G, Wu NH, Nitsche A, Müller MA, Drosten C, Pöhlmann S. 2020. SARS-CoV-2 cell entry depends on ACE2 and TMPRSS2 and is blocked by a clinically proven protease inhibitor. Cell 181:271-280.

5. Thevarajan I, Nguyen THO, Koutsakos M, Druce J, Caly L, van de Sandt CE, Jia X, Nicholson S, Catton M, Cowie B, Tong SYC, Lewin SR, Kedzierska K. 2020. Breadth of concomitant immune responses prior to patient recovery: a case report of non-severe COVID-19. Nat Med 26:453-455.

6. Gao, Q, Bao L, Mao H, Wang L, Xu K, Yang M, Li Y, Zhu L, Wang N, Lv Z, Gao H, Ge X, Kan B, Hu Y, Jiangning Liu J, Cai F, Jiang D, Yin Y, Qin C, Li J, Gong X, Lou X, Shi W, Wu D, Zhang H, Zhu L, Deng W, Li Y, Lu J, Li C, Wang X, Yin W,

499 Zhang Y, Qin C. 2020. Development of an inactivated vaccine candidate for
500 SARS-CoV-2. Science 369:77-81.
501 7. Guebre-Xabier M, Patel N, Tian J-H, Zhou B, Maciejewski S, Lam K, Portnoff AD,
502 Massare MJ, Frieman MB, Piedra PA, Ellingsworth L, Glenn G, Gale Smith G.
503 2020. NVX-CoV2373 vaccine protects cynomolgus macaque upper and lower
504 airways against SARS-CoV-2 challenge. bioRxiv
505 https://doi.org/10.1101/2020.08.18.256578.
506 8. Walsh EE, Frenck R, Falsey AR, Kitchin N, Absalon J, Gurtman A, Lockhart S,
507 Neuzil K, Mulligan MJ, Bailey R, Swanson KA, Li P, Koury K, Kalina W, Cooper
508 D, Fontes-Garfias C, Shi P-Y, Türeci Z, Tompkins KR, Lyke KE, Raabe V,
509 Dormitzer PR, Jansen KU, Şahin U, Gruber WC. 2020. RNA-based COVID-19
510 vaccine BNT162b2 selected for a pivotal efficacy study. medRxiv
511 https://doi.org/10.1101/2020.08.17.20176651.
512 9. Yu J, Tostanoski LH, Peter L, Mercado NB, McMahan K, Mahrokhian SH, Nkolola
513 JP, Liu J, Li Z, Chandrashekar A, Martinez DR, Loos C, Atyeo C, Fischinger S,
514 Burke JS, Slein MD, Chen Y, Zuiani A, Lelis FJN, Travers M, Habibi S, Pessaint L,
515 Ry AV, Blade K, Brown R, Cook A, Finneyfrock B, Dodson A, Teow E, Velasco J,
516 Zahn R, Wegmann F, Bondzie EA, Dagotto G, Gebre MS, He X, Jacob-Dolan C,
517 Kirilova M, Kordana N, Lin Z, Maxfield LF, Nampanya F, Nityanandam R, Ventura
518 JD, Wan H, Cai Y, Chen B, Schmidt AG, Wesemann DR, Baric RS, Alter G,

519 Andersen H, Lewis MG, Barouch DH. 2020. DNA vaccine protection against
520 SARS-CoV-2 in rhesus macaques. Science 369:806-811.
521 10. Hassan AO, Kafai NM, Dmitriev IP, Fox JM, Smith BK, Harvey IB, Chen RE,
522 Winkler ES, Wessel AW, Case JB, Kashentseva E, McCune BT, Bailey AL, Zhao
523 H, VanBlargan LA, Dai Y-N, Ma M, Adams LJ, Shrihari S, Danis JE, Gralinski LE,
524 Hou YJ, Schäfer A, Kim AS, Keeler SP, Weiskopf D, Baric RS, Holtzman MJ,
525 Fremont DH, Curiel DT, Diamond MS. 14 August 2020. A single-dose intranasal
526 ChAd vaccine protects upper and lower respiratory tracts against SARS-CoV-2.
527 Cell https://doi.org/10.1016/j.cell.2020.08.026
528 11. Iwasaki A, Yang Y. 2020. The potential danger of suboptimal antibody responses in
529 COVID-19. Nat Rev Immunol 20:339-341.
530 12. Arvin AM, Fink K, Schmid MA, Cathcart A, Spreafico R, Havenar-Daughton C,
531 Lanzavecchia A, Corti D, Virgin HW. 2020. A perspective on potential
532 antibody-dependent enhancement of SARS-CoV-2. Nature 584:353-363.
533 13. Weingart H, Czub M, Czub S, Neufeld J, Marszal P, Gren J, Smith G, Jones S,
534 Proulx R, Deschambault Y, Grudeski E, Andonov A, He R, Li Y, Copps J, Grolla A,
535 Dick D, Berry J, Ganske S, Manning L, Cao J. 2004. Immunization with modified
536 vaccinia virus Ankara-based recombinant vaccine against severe acute respiratory
537 syndrome is associated with enhanced hepatitis in ferrets. J Virol 78:12672-12676.
538 14. Tseng CT, Sbrana E, Iwata-Yoshikawa N, Newman PC, Garron T, Atmar RL, Peters
539 CJ, Couch RB. 2012. Immunization with SARS coronavirus vaccines leads to

pulmonary immunopathology on challenge with the SARS virus. PLoS One 7:e35421.

15. Wang SF, Tseng SP, Yen CH, Yang JY, Tsao CH, Shen CW, Chen KH, Liu FT, Liu WT, Chen YM, Huang JC. 2014. Antibody-dependent SARS coronavirus infection is mediated by antibodies against spike proteins. Biochem Biophys Res Commn 451:208-214.

16. Liu L, Wei Q, Lin Q, Fang J, Wang H, Kwok H, Tang H, Nishiura K, Peng J, Tan Z, Wu T, Cheung K-W, Chan K-H, Alvarez X, Qin C, Lackner A, Perlman S, Yuen K-Y, Chen Z. 2019. Anti-spike IgG causes severe acute lung injury by skewing macrophage responses during acute SARS-CoV infection. JCI Insight 4:e123158.

17. Robbiani DF, Gaebler C, Muecksch F, Lorenzi JCC, Wang Z, Cho A, Agudelo M, Barnes CO, Gazumyan A, Finkin S, Hägglöf T, Oliveira TY, Viant C, Hurley A, Hoffmann HH, Millard KG, Kost RG, Cipolla M, Gordon K, Bianchini F, Chen ST, Ramos V, Patel R, Dizon J, Shimeliovich I, Mendoza P, Hartweger H, Nogueira L, Pack M, Horowitz J, Schmidt F, Weisblum Y, Michailidis E, Ashbrook AW, Waltari E, Pak JE, Huey-Tubman KE, Koranda N, Hoffman PR, West AP Jr, Rice CM, Hatziioannou T, Bjorkman PJ, Bieniasz PD, Caskey M, Nussenzweig MC. 2020. Convergent antibody responses to SARS-CoV-2 in convalescent individuals. Nature 584:437-442.

18. Juno JA, Tan H-X, Lee WS, Reynaldi A, Kelly HG, Wragg K, Esterbauer R, Kent HE, Batten J, Mordant FL, Gherardin NA, Pymm P, Dietrich MH, Scott NE, Tham

W-H, Godfrey DI, Subbarao K, Davenport MP, Kent SJ, Wheatley AK. 13 July 2020. Humoral and circulating follicular helper T cell responses in recovered patients with COVID-19. https//doi.org/10.1038/s41591-020-0995-0.

19. Pinto D, Park Y-J, Beltramello M, Walls AC, Tortorici A, Bianchi S, Jaconi S, Culap K, Zatta F, De Marco, A, Peter A, Guarino B, Spreafico R, Cameroni E, Case JB, Chen RE, Havenar-Daughton C, Snell G, Telenti A, Virgin HW, Lanzavecchia A, Diamond MS, Fink K, Veesler D, Corti D. 2020. Cross-neutralization of SARS-COV-2 by a human monoclonal SARS-CoV antibody. Nature 583:290-295.

20. Liu L, Wang P, Nair MS, Yu J, Rapp M, Wang Q, Luo Y, Chan JF-W, Sahi V, Figueroa A, Guo XV, Cerutti G, Bimela J, Gorman J, Zhou T, Chen Z, Yuen K-W, Kwong PD, Sodroski JG, Yin MT, Sheng Z, Huang Y, Shapiro L, Ho DD. 2020. Potent neutralizing antibodies against multiple epitopes on SARS-CoV-2 spike. Nature 584: 450-456.

21. Zost SJ, Gilchuk P, Case JB, Binshtein E, Chen RE, Nkolola JP, Schäfer A, Reidy JX, Trivette A, Nargi RS, Sutton RE, Suryadevara N, Martinez DR, Williamson LE, Chen EC, Jones T, Day S, Myers L, Hassan AO, Kafai NM, Winkler ES, Fox JM, Shrihari S, Mueller BK, Meiler J, Chandrashekar A, Mercado NB, Steinhardt JJ, Ren K, Loo Y-M, Kallewaard NL, McCune BT, Keeler SP, Holtzman MJ, Barouch DH, Gralinski LE, Baric RS, Thackray LB, Diamond MS, Carnahan RH, Crowe Jr JE. 2020. Potently neutralizing and protective human antibodies against SARS-CoV-2. Nature 584: 443-449.

582 22. Ledford H. 2020. Antibody therapies could be a bridge to a coronavirus vaccine-but
583 will the world benefit? Nature 584:333-334.
584 23. Cao W-C, Liu W, Zhang P-H, Zhang F, Richardus JH. 2007. Disappearance of
585 antibodies to SARS-associated coronavirus after recovery. N Engl J Med
586 357:1162-1163.
587 24. Mo H, Zeng G, Ren X, Li H, Ke C, Tan Y, Cai C, Lai K, Chen R, Chan-Yeung M,
588 Zhong N. 2006. Longitudinal profile of antibodies against SARS-coronavirus in
589 SARS patients and their clinical significance. Respirology 11:49-53.
590 25. Ng OW, Chia A, Tan AT, Jadi RS, Leong HN, Bertoletti A, Tan YJ. 2016. Memory
591 T cell responses targeting the SARS coronavirus persist up to 11 years
592 post-infection. Vaccine 34:2008-2014.
593 26. Seow J, Graham C, Merrick B, Acors S, Steel KJA, Hemmings O, O'Bryne A,
594 Kouphou N, Pickering S, Galao RP, Betancor G, Wilson HD, Signell AW, Winstone
595 H, Kerridge C, Temperton N, Snell L, Bisnauthsing K, Moore A, Green A, Martinez
596 L, 6 , Stokes B, Honey J, Izquierdo-Barras A, Arbane G, Patel A, O'Connell L,
597 O'Hara G, MacMahon E, Douthwaite S, Nebbia G, Batra R, Martinez-Nunez R,
598 Edgeworth JD, Neil1 SJD, Malim MH, Doores KJ. 2020. Logitudinal evaluation and
599 decline of antibody responses in SARS-CoV-2 infection. medRxiv
600 https://doi.org/10.1101/2020.07.09.20148429.
601 27. Diao B, Wang C, Tan Y, Chen X, Liu Y, Ning L, Chen L, Li M, Liu Y, Wang G,
602 Yuan Z, Feng Z, Zhang Y, Wu Y, Chen Y. 2020. Reduction and functional

exhaustion of T cells in patients with coronavirus disease 2019 (COVID-19). Front immunol 11:1729. https://doi.rog/10.3389/fimmu.2020.01729.

28. Lucas C, Wong P, Klein J, Castro TBR, Silva J, Sundaram M, Ellingson MK, Mao T, Oh JE, Israelow B, Takahashi T, Tokuyama M, Lu P, Venkataraman A, Park A, Mohanty S, Wang H, Wyllie AL, Vogels CBF, Earnest R, Lapidus S, Ott IM, Moore AJ, Muenker MC, Fournier JB, Campbell M, Odio CD, Casanovas-Massana A; Yale IMPACT Team, Herbst R, Shaw AC, Medzhitov R, Schulz WL, Grubaugh ND, Dela Cruz C, Farhadian S, Ko AI, Omer SB, Iwasaki A. 2020. Longitudinal analyses reveal immunological misfiring in severe COVID-19. Nature 584: 463-469.

29. Cui J, Li F, Shi ZL. Origin and evolution of pathogenic coronaviruses. 2019. Nat Rev Microbiol 17:181-192.

30. Kohyama S, Ohno S, Tatsuya Suda T, Taneichi M, Yokoyama S, Mori M, Kobayashi A, Hayashi H, Tetsuya Uchida T, Matsui M. 2009. Efficient induction of cytotoxic T lymphocytes specific for severe acute respiratory syndrome (SARS)-associated coronavirus by immunization with surface-linked liposomal peptides derived from a non-structural polyprotein 1a. Antiviral Res 84:168-177.

31. Rammensee H, Bachmann J, Emmerich NP, Bachor OA, Stevanović S. 1999. SYFPEITHI: database for MHC ligands and peptide motifs. Immunogenetics 50:213-219.

32. Bhasin M, Raghava GPS. 2006. A hybrid approach for predicting promiscuous MHC class I restricted T cell epitopes. J Biosci 32:31-42.

624 33. Singh H, Raghava GPS. 2003. ProPred1: Prediction of promiscuous MHC class-I
625 binding sites. Bioinformatics 19:1009-1014.
626 34. Vita R, Mahajan S, Overton JA, Dhanda SK, Martini S, Cantrell JR, Wheeler DK,
627 Sette A, Peters B. 2019. The immune epitope database (IEDB): 2018
628 update. Nucleic Acids Res 47(D1):D339-D343.
629 https://doi.org/10.1093/nar/gky1006.
630 35. Gotch F, Rothbard J, Howland K, Townsend A, McMichael A. 1987. Cytotoxic T
631 lymphocytes recognize a fragment of influenza virus matrix protein in association
632 with HLA-A2. Nature 326:881-882.
633 36. Tsomides TJ, Walker BD, Eisen HN. 1991. An optimal viral peptide recognized by
634 $CD8^+$ T cells binds very tightly to the restricting class I major histocompatibility
635 complex protein on intact cells but not to the purified class I protein. Proc Natl
636 Acad Sci U S A 88:11276-11280.
637 37. Pascolo S, Bervas N, Ure JM, Smith AG, Lemonnier FA, Pérarnau B. 1997.
638 HLA-A2.1-restricted education and cytolytic activity of $CD8^+$ T lymphocytes from
639 beta2 microglobulin (beta2m) HLA-A2.1 monochain transgenic H-$2D^b$ beta2m
640 double knockout mice. J Exp Med 185:2043-2051.
641 38. Grifoni A, Sidney J, Zhang Y, Scheuermann RH, Peters B, Sette A. 2020. A
642 sequence homology and bioinformatics approach can predict candidate targets for
643 immune responses to SARS-CoV-2. Cell Host & Microbe 27:671-680, 2020.

644 39. Ong E, Wong MU, Huffman A, He Y. COVID-19 coronavirus vaccine design using
645 reverse vaccinology and machine learning. Front Immunol 11:1581.
646 https://doi.org/10.3389/fimmu.2020.01581.
647 40. Le Bert N, Tan AT, Kunasegaran K, Tham CYL, Hafezi M, Chia A, Chng MHY, Lin
648 M, Tan N, Linster M, Chia WN, Chen MI, Wang LF, Ooi EE, Kalimuddin S,
649 Tambyah PA, Low JG, Tan YJ, Bertoletti A. 2020. SARS-CoV-2-specific T cell
650 immunity in cases of COVID-19 and SARS, and uninfected controls. Nature
651 584:457-462.
652 41. Mateus J, Grifoni A, Tarke A, John Sidney J, Ramirez SI, Dan JM, Burger ZC,
653 Rawlings SA, Smith DM, Phillips E, Mallal S, Lammers M, Rubiro P, Quiambao L,
654 Sutherland A, Yu ED, Antunes RS, Greenbaum J, Frazier A, Markmann AJ,
655 Premkumar L, de Silva A, Peters B, Crotty S, Sette A, Weiskopf D. 2020. Selective
656 and cross-reactive SARS-CoV-2 T cell epitopes in unexposed humans. Science 4
657 August 2020. eabd3871. https://doi.org/10.1126/science.abd3871.
658 42. Grifoni A,Weiskopf D, Ramirez SI, Mateus J, Dan JM, Moderbacher CR, Rawlings
659 SA, Sutherland A, Premkumar L, Jadi RS, Marrama D, de Silva AM, Frazier A,
660 Carlin AF, Greenbaum JA, Peters B, Krammer F,Smith DM, Crotty S,1,2,5, Sette A.
661 2020. Targets of T cell responses to SARS-CoV-2 coronavirus in humans with
662 COVID-19 disease and unexposed individuals. Cell 181:1489-1501.
663 43. Braun J, Loyal L, Frentsch M, Wendisch D, Georg P, Kurth F, Hippenstiel S,
664 Dingeldey M, Kruse B, Fauchere F, Baysal E, Mangold M, Henze L, Lauster R,

Mall MA, Beyer K, Röhmel J, Voigt S, Schmitz J, Miltenyi S, Demuth I, Müller MA, Hocke A, Witzenrath M, Suttorp N, Kern F, Reimer U, Wenschuh H, Drosten C, Corman VM, Giesecke-Thiel C, Sander LE, Thiel A. 2020. SARS-CoV-2-reactive T cells in healthy donors and patients with COVID-19. Nature https://doi.org/10.1038/s41586-020-2598-9.

44. Nelde A, Bilich T, Heitmann JS, Maringer Y, Salih HR, Roerden M, Lübke M, Bauer J, Jonas Rieth J, Wacker M, Peter A, Hörber S, Traenkle B, Kaiser PD, othbauer U, Becker M, Junker D, Krause G, Strengert M, Schneiderhan-Marra N, Templin MF, Joos TO, Kowalewski DJ, Stos-Zweifel V, Fehr M, Graf M, Gruber L-C, Rachfalski D, Preuß B, Hagelstein I, Märklin M, Bakchoul T, Gouttefangeas C, Kohlbacher O, Klein R, Stevanović S, Rammensee H-G, Walz JS. 2020. SARS-CoV-2-epitopes define heterologous and COVID-19-induced T-cell recognition. Research Square http://doi.org/10.21203/rs.3.rs-35331/v1.

45. Sette A, Crotty, S. 2020. Pre-existing immunity to SARS-CoV-2: the knowns and unknowns. Nat Rev Immunol 20:457-458.

46. Matsui M, Kawano M, Matsushita S, Akatsuka T. 2014. Introduction of a point mutation into an HLA class I single-chain trimer induces enhancement of CTL priming and antitumor immunity. Mol Ther Methods Clin Dev 1:14027. https://doi.org/10.1038/mtm.2014.27.

684 47. Parham, P and Brodsky, FM. 1981. Partial purification and some properties of
685 BB7.2. A cytotoxic monoclonal antibody with specificity for HLA-A2 and a variant
686 of HLA-A28. Hum Immunol 3: 277-299.
687

688 **Figure legends**

689 **Fig. 1.** The linear diagrams of the SARS-CoV-2 genome and the protein subunits of
690 ORF1a. The SARS-CoV-2 genome consists of ORF1a, ORF1b, Spike (S), ORF3a,
691 Envelope (E), Membrane (M), ORF6, ORF7a, ORF7b, ORF8, Nucleocapsid (N), and
692 ORF10. The ORF1a polyprotein is composed of eleven non-structural proteins,
693 nsp1-nsp11.

694

695 **Fig. 2.** Intracellular IFN-γ staining of $CD8^+$ T cells specific for peptides derived from
696 SARS-CoV-2 pp1a. HHD mice were immunized twice with each of predicted peptides of
697 SARS-CoV-2 pp1a in liposomes together with CpG. After one week, spleen cells were
698 prepared and stimulated with (+) or without (-) a relevant peptide for 5 hours. Cells were
699 then stained for their surface expression of CD8 (x axis) and their intracellular expression
700 of IFN-γ (y axis). The numbers shown indicate the percentages of intracellular IFN-γ^+
701 cells within $CD8^+$ T cells. Three to five mice per group were used in each experiment,
702 and the spleen cells of the mice per group were pooled.

703

704 **Fig. 3.** (A) *In vivo* killing activities specific for the 10 peptides. HHD mice were
705 immunized twice with either each of the 10 liposomal peptides (pp1a-38, -84, -641,
706 -1675, -2884, -3467, -3583, -3662, 3710, and -3732) or liposomes alone together with
707 CpG. One week later, *in vivo* peptide-specific killing activities were measured. Three to
708 five mice per group were used, and the data of % specific lysis are shown as the mean ±

709 SD. (B & C) Comparison of the 10 peptides in the induction of IFN-γ^+ $CD8^+$ T cells.
710 Seventeen HHD mice were immunized once with the mixture of 10 peptides involving
711 pp1a-38, -84, -641, -1675, -2884, -3467, -3583, -3662, -3710, and -3732 in liposomes
712 with CpG. After one week, spleen cells were stimulated with or without each of the 10
713 peptides, and intracellular IFN-γ in CD8+ T cells was stained. (C) Y-axis indicates the
714 relative percentages of IFN-γ^+ cells in $CD8^+$ T cells which were calculated by subtracting
715 the % of IFN-γ^+ cells in $CD8^+$ T cells without a peptide from the % of IFN-γ^+ cells in
716 $CD8^+$ T cells with a relevant peptide. Each blue circle represents an individual mouse.
717 Data are shown as the mean (horizontal bars) ± SD. (B) Statistical comparisons of the
718 relative % values of IFN-γ^+ $CD8^+$ T cells among the 10 peptides in Fig. 3C were made by
719 one-way ANOVA followed by post-hoc tests. *, $P < 0.05$; **, $P < 0.01$; ***, $P < 0.001$;
720 ns, not significant.
721
722 **Fig. 4.** Comparison of the 10 peptides in the induction of $CD107a^+$ $CD8^+$ T cells (A) and
723 $CD69^+$ $CD8^+$ T cells (B). Nine HHD mice were immunized once with the mixture of 10
724 peptides involving pp1a-38, -84, -641, -1675, -2884, -3467, -3583, -3662, -3710, and
725 -3732 in liposomes with CpG. After one week, spleen cells were stimulated with or
726 without each of the 10 peptides, and the expression of CD107a (A) or CD69 (B) on CD8+
727 T cells was analyzed. Data indicates the relative percentages of $CD107a^+$ (A) and $CD69^+$
728 (B) cells in $CD8^+$ T cells which were obtained by subtracting the % of $CD107a^+$ and
729 $CD69^+$ cells in $CD8^+$ T cells without a peptide from the % of $CD107a^+$ and $CD69^+$ cells

730 in $CD8^+$ T cells with a peptide, respectively. Each red (A) or green (B) circle represents
731 an individual mouse. Data are shown as the mean (horizontal bars) ± SD. Statistical
732 analyses of the data among the 10 peptides in Fig. 4A and Fig. 4B were performed by
733 one-way ANOVA followed by post-hoc tests in Fig. 4C and Fig 4D, respectively. *, $P <$
734 0.05; **, $P < 0.01$; ***, $P < 0.001$; ns, not significant.
735
736 **Fig. 5.** Three types of reactivity in mice immunized with the mixture of the 10 peptides.
737 Fifteen mice were immunized once with the mixture of 10 peptides including pp1a-38,
738 -84, -641, -1675, -2884, -3467, -3583, -3662, -3710, and -3732 in liposomes with CpG.
739 After one week, spleen cells were stimulated with or without each of the 10 peptides, and
740 intracellular IFN-γ in CD8+ T cells was stained. Based on the reactivity pattern to the 10
741 peptides, fifteen mice were divided into three types, A-C. Each graph represents
742 reactivity of an individual mouse. Y-axis indicates the relative percentage of IFN-γ^+ cells
743 in $CD8^+$ T cells which was calculated by subtracting the % of IFN-γ^+ cells in $CD8^+$ T
744 cells without a peptide from the % of IFN-γ^+ cells in $CD8^+$ T cells with a relevant peptide.
745 Statistical analyses of the relative % values to 10 peptides in each type were performed by
746 one-way ANOVA followed by post-hoc tests. *, $P < 0.05$; **, $P < 0.01$; ***, $P < 0.001$;
747 ns, not significant.
748

Table 1. Predicted CTL epitopes for the SARS-CoV-2 non-structural polyprotein 1a

High binders					
Name	Sequence	BL_{50}	Name	Sequence	BL_{50}
pp1a-84	VMVELVAEL	6.8 ± 0.3	pp1a-103	TLGVLVPHV	1.3 ± 0.2
pp1a-214	TLSEQLDFI	2.0 ± 0.2	pp1a-445	GLNDNLLEI	6.0 ± 0.2
pp1a-597	VMAYITGGV	9.5 ± 0.9	pp1a-619	TVYEKLKPV	5.6 ± 0.7
pp1a-641	FLRDGWEIV	0.9 ± 0.1	pp1a-1675	YLATALLTL	8.4 ± 0.2
pp1a-2270	YLNSTNVTI	8.9 ± 0.3	pp1a-2569	ILLLDQALV	9.6 ± 1.5
pp1a-2785	AIFYLITPV	5.1 ± 1.6	pp1a-2968	YLEGSVRVV	7.5 ± 0.1
pp1a-3013	SLPGVFCGV	3.1 ± 0.2	pp1a-3115	YLTNDVSFL	4.8 ± 0.3
pp1a-3122	FLAHIQWMV	6.9 ± 0.4	pp1a-3128	WMVMFTPLV	9.8 ± 1.1
pp1a-3587	ILTSLLVLV	8.3 ± 0.9	pp1a-3710	TLMNVLTLV	2.0 ± 0.4
pp1a-3732	SMWALIISV	8.9 ± 0.4	pp1a-4094	ALWEIQQVV	6.4 ± 0.4
Medium binders					
Name	Sequence	BL_{50}	Name	Sequence	BL_{50}
pp1a-15	QLSLPVLQV	79.4 ± 4.4	pp1a-38	VLSEARQHL	76.8 ± 6.8
pp1a-52	GLVEVEKGV	14.5 ± 4.9	pp1a-106	VLVPHVGEI	76.0 ± 2.0
pp1a-468	KLNEEIAII	56.2 ± 4.8	pp1a-600	YITGGVVQL	48.5 ± 7.9
pp1a-685	FLALCADSI	10.2 ± 0.5	pp1a-702	ALNLGETFV	40.7 ± 2.8
pp1a-1109	NLAKHCLHV	38.5 ± 8.2	pp1a-1114	CLHVVGPNV	62.9 ± 2.3
pp1a-1161	SLRVCVDTV	85.7 ± 1.9	pp1a-1312	MLAKALRKV	95.2 ± 0.7
pp1a-2168	YMPYFFTLL	99.0 ± 2.4	pp1a-2332	ILFTRFFYV	96.5 ± 14.0
pp1a-2563	QLMCQPILL	11.1 ± 1.8	pp1a-2884	FLPRVFSAV	29.3 ± 6.5
pp1a-3047	IVAGGIVAI	50.5 ± 2.5	pp1a-3083	LLFLMSFTV	39.4 ± 0.9
pp1a-3183	FLLNKEMYL	12.9 ± 6.8	pp1a-3403	FLNGSCGSV	18.7 ± 3.2
pp1a-3467	VLAWLYAAV	45.0 ± 10.8	pp1a-3475	VINGDRWFL	85.0 ± 5.4
pp1a-3482	FLNRFTTTL	79.0 ± 9.6	pp1a-3583	LLLTILTSL	63.8 ± 3.1
pp1a-3639	FLLPSLATV	15.0 ± 4.4	pp1a-3662	RIMTWLDMV	76.5 ± 7.1
pp1a-3753	FLARGIVFM	71.2 ± 12.9	pp1a-3798	CLLNRYFRL	81.6 ± 20.2
pp1a-3807	TLGVYDYLV	61.7 ± 8.7	pp1a-3871	VLLSVLQQL	44.9 ± 6.0
pp1a-3886	KLWAQCVQL	27.2 ± 9.4	pp1a-4183	ALLSDLQDL	42.4 ± 6.1
pp1a-4266	VLSFCAFAV	20.1 ± 6.1	pp1a-4283	YLASGGQPI	39.8 ± 6.2
Low binders					
Name	Sequence	BL_{50}	Name	Sequence	BL_{50}
pp1a-572	GISQYSLRL	ND	pp1a-589	DLATNNLVV	ND
pp1a-692	SIIIGGAKL	ND	pp1a-881	KTLQPVSEL	161.7 ± 28.3
pp1a-1143	VLLAPLLSA	ND	pp1a-1148	LLSAGIFGA	ND
pp1a-1214	FITESKPSV	122.1 ± 31.7	pp1a-1367	ILGTVSWNL	123.2 ± 11.3
pp1a-1387	KLMPVCVET	174.2 ± 33.5	pp1a-1433	SLINTLNDL	123.4 ± 11.0
pp1a-1642	FLGRYMSAL	124.1 ± 1.9	pp1a-1962	DLNGDVVAI	ND
pp1a-2076	ILKPANNSL	ND	pp1a-2226	LINIIIWFL	ND
pp1a-2228	NIIIWFLLL	ND	pp1a-2230	IIWFLLLSV	176.7 ± 6.3
pp1a-2235	LLSVCLGSL	ND	pp1a-2242	SLIYSTAAL	134.0 ± 7.6
pp1a-2249	ALGVLMSNL	ND	pp1a-2348	QLFFSYFAV	146.4 ± 19.7
pp1a-2363	WLMWLIINL	102.7 ± 6.4	pp1a-2364	LMWLIINLV	159.0 ± 42.8
pp1a-2901	KLIEYTDFA	126.0 ± 2.5	pp1a-3344	SMQNCVLKL	104.5 ± 2.2
pp1a-3827	GLLPPKNSI	ND	pp1a-3839	KLNIKLLGV	213.5 ± 85.7
pp1a-3917	VLLSMQGAV	112.3 ± 7.2	pp1a-4032	MLFTMLRKL	165.8 ± 21.7

Data of peptide binding assays are shown as BL_{50}, indicating a concentration (μM) of each peptide that yields the 50% relative binding as shown in the materials and methods. Experiments were performed in triplicate and repeated twice with similar results. Data are given as mean values ± SD. High binders: $BL_{50} < 10$ μM; Medium binders: $10\ \mu M \leq BL_{50} < 100\ \mu M$; Low binders: $BL_{50} \geq 100$ μM or ND (not detected).

Table 2
Comparison of amino acid sequences of SARS-CoV-2 pp1a CTL epitopes with the amino acid sequence of SARS-CoV

SARS-CoV-2				SARS-CoV	
Name	Start-End	Sequence	Protein	Sequence	Identity (%)
pp1a-38	38-46	VLSEARQHL	nsp1	ALSEAREHL	89
pp1a-52	52-60	GLVEVEKGV	nsp1	GLVELEKGV	89
pp1a-84	84-92	VMVELVAEL	nsp1	KVVELVAEM	67
pp1a-103	103-11	TLGVLVPHV	nsp1	TLGVLVPHV	100
pp1a-445	445-53	GLNDNLLEI	nsp2	TLNEDLLEI	67
pp1a-597	597-605	VMAYITGGV	nsp2	IMAYVTGGL	67
pp1a-641	641-9	FLRDGWEIV	nsp2	FLKDAWEIL	67
pp1a-1675	1675-83	YLATALLTL	nsp3		
pp1a-2785	2785-93	AIFYLITPV	nsp4		
pp1a-2884	2884-92	FLPRVFSAV	nsp4	FLPRVFSAV	100
pp1a-3083	3083-91	LLFLMSFTV	nsp4	LLFLMSFTI	89
pp1a-3403	3403-11	FLNGSCGSV	nsp5	FLNGSCGSV	100
pp1a-3467	3467-75	VLAWLYAAV	nsp5	VLAWLYAAV	100
pp1a-3583	3583-91	LLLTILTSL	nsp6		
pp1a-3662	3662-70	RIMTWLDMV	nsp6	RIMTWLELA	67
pp1a-3710	3710-8	TLMNVLTLV	nsp6	TLMNVITLV	89
pp1a-3732	3732-40	SMWALIISV	nsp6	SMWALVISV	89
pp1a-3886	3886-94	KLWAQCVQL	nsp7		

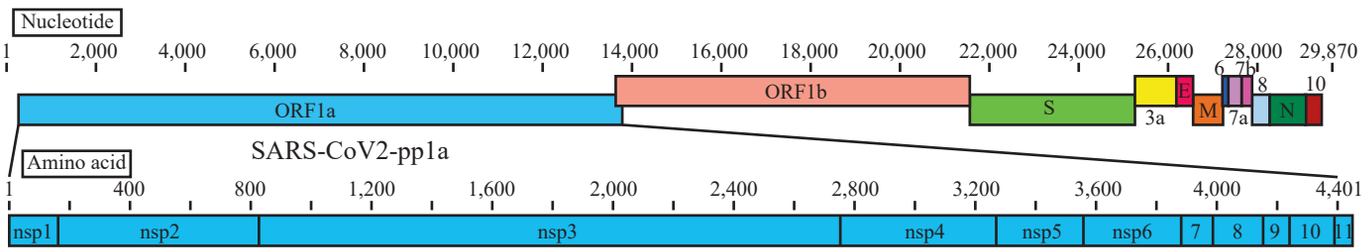

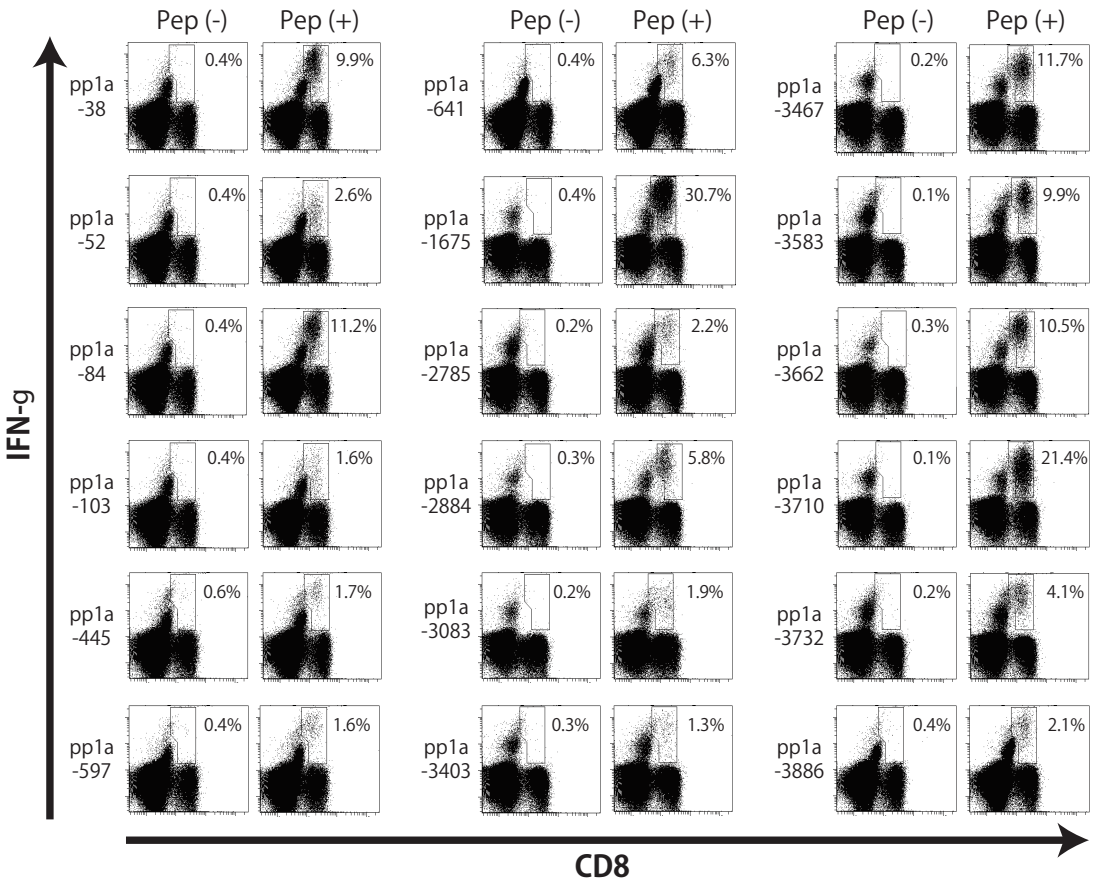
Pep (-)
Pep (+)
Pep (-)
Pep (+)
Pep (-)
Pep (+)
pp1a -38
0.4%
9.9%
pp1a -641
0.4%
6.3%
pp1a -3467
0.2%
11.7%
pp1a -52
0.4%
2.6%
pp1a -1675
0.4%
30.7%
pp1a -3583
0.1%
9.9%
pp1a -84
0.4%
11.2%
pp1a -2785
0.2%
2.2%
pp1a -3662
0.3%
10.5%
pp1a -103
0.4%
1.6%
pp1a -2884
0.3%
5.8%
pp1a -3710
0.1%
21.4%
pp1a -445
0.6%
1.7%
pp1a -3083
0.2%
1.9%
pp1a -3732
0.2%
4.1%
pp1a -597
0.4%
1.6%
pp1a -3403
0.3%
1.3%
pp1a -3886
0.4%
2.1%
IFN-g
CD8

A

Name	% Specific Lysis
pp1a-38	78.2 ± 15.0
pp1a-84	92.2 ± 6.7
pp1a-641	78.9 ± 16.2
pp1a-1675	84.6 ± 11.0
pp1a-2884	77.9 ± 7.5
pp1a-3467	83.8 ± 6.7
pp1a-3583	86.8 ± 15.9
pp1a-3662	87.3 ± 5.4
pp1a-3710	80.2 ± 10.3
pp1a-3732	88.6 ± 5.8

B

	38	84	641	1675	2884	3467	3583	3662	3710	3732
38	—	ns	ns	***	***	**	***	***	ns	ns
84		—	ns	***	***	***	***	***	*	ns
641			—	*	ns	ns	*	ns	ns	ns
1675				—	ns	ns	ns	ns	ns	*
2884					—	ns	ns	ns	ns	ns
3467						—	ns	ns	ns	ns
3583							—	ns	ns	*
3662								—	ns	*
3710									—	ns
3732										—

C

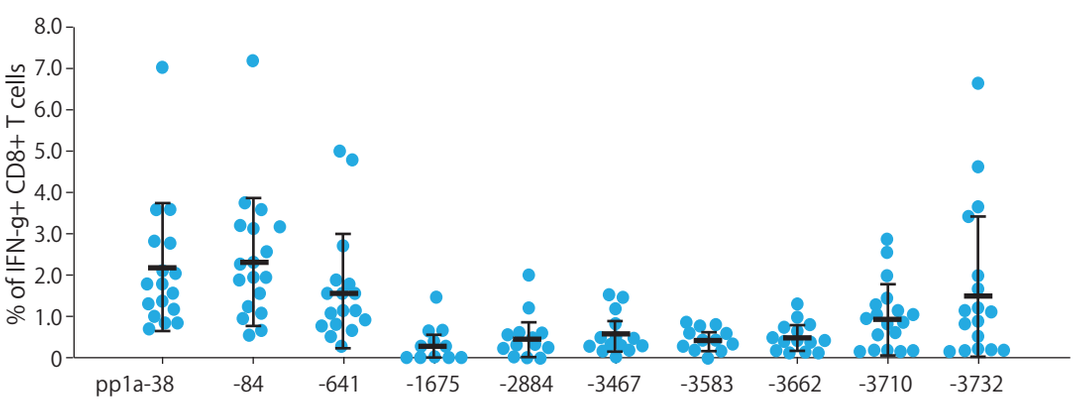

A

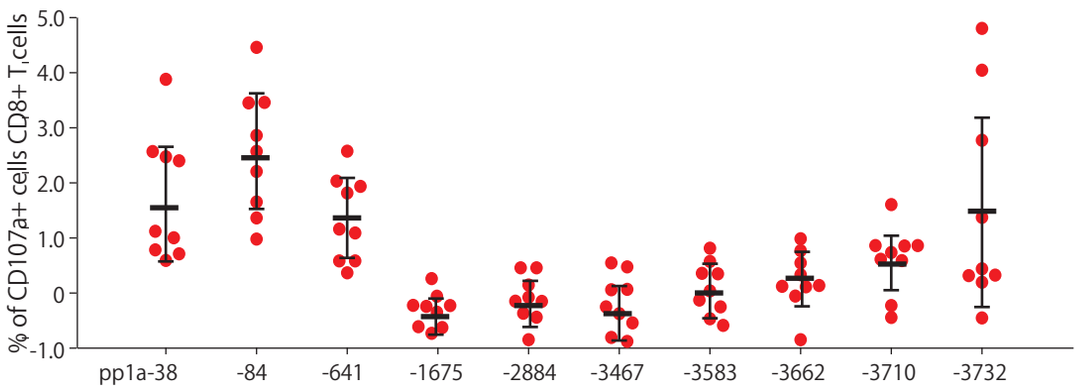

B

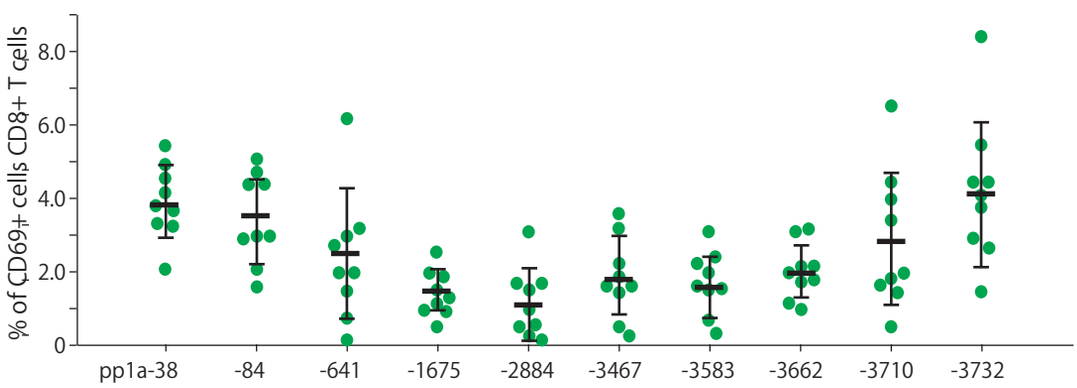

C

	38	84	641	1675	2884	3467	3583	3662	3710	3732
38	—	ns	ns	***	**	**	*	*	ns	ns
84		—	ns	***	***	***	***	***	***	ns
641			—	**	*	*	ns	ns	ns	ns
1675				—	ns	ns	ns	ns	ns	**
2884					—	ns	ns	ns	ns	*
3467						—	ns	ns	ns	**
3583							—	ns	ns	*
3662								—	ns	ns
3710									—	ns
3732										—

D

	38	84	641	1675	2884	3467	3583	3662	3710	3732
38	—	ns	ns	**	***	*	*	ns	ns	ns
84		—	ns	*	*	ns	ns	ns	ns	ns
641			—	ns	ns	ns	ns	ns	ns	ns
1675				—	ns	ns	ns	ns	ns	**
2884					—	ns	ns	ns	ns	***
3467						—	ns	ns	ns	**
3583							—	ns	ns	**
3662								—	ns	*
3710									—	ns
3732										—